Modeling of a synthetic presalt 2D seismic dataset representative of offshore East margin basins (Brazil) – preliminary results

Alexandre de Souza Oliveira, Agência Nacional do Petróleo (ANP)/SEP, Brazil
Carlos A. S. Ferreira, Agência Nacional do Petróleo (ANP)/SEP, Brazil

Abstract

The offshore East margin basins, especially Campos, Santos and Espírito Santo, are the main oil producers in siliciclastics reservoirs in Brazil. However, in recent times large volumes of light oil in carbonate reservoirs in the Aptian presalt section in Santos (BM-S-11, Tupi prospect) have also called the attention of the oil industry due to its potential hydrocarbon content. To the geophysical community, imaging this kind of reservoir represents a new exploration frontier in its characterization and its seismic signature. The main challenge here is the imaging under salt followed by the mapping of amplitude anomalies (e.g., AVO) related to carbonate reservoirs, which are extremely anisotropic in nature. This paper then presents the results of a simple modeling of a representative offshore presalt prospect considering its main geological characteristics.

Introduction

Almost all tectonic, structural and stratigraphic knowledge of the Brazilian offshore sedimentary basins are based on the processing and interpretation of 2D/3D seismic, potential (gravimetric and magnetometric) and wellbore data. The geologic interpretation of these dataset suggests a tectonic and sedimentary evolution that spans through the Cretaceous to the Tertiary (i.e., about 140 million years old), including important geologic formation processes of the South America and Africa continents, the genesis of the South Atlantic Ocean and the formation of the oceanic crust. This geological scenario represents one of the most prolific oil provinces in the world, object of great strategic and political interests due to recent discoveries of giant hydrocarbons reserves (i.e., BM-S-11, Tupi prospect) in the presalt section of Santos basin. The precise knowledge of the petroleum system occurring along not only in Santos but also along the other East margin basins, the characterization of exploratory plays and prospects, is an important frontier, the latter one direct related to the technologic frontiers (e.g., in seismic imaging) to be implemented in the exploration of these non-conventional resources.

In this paper we describe the results of the modeling of a simple 2D seismic dataset of a representative presalt model derived from any of the Brazil East margin offshore basins (**Figure 1**). Our objective here is to assess the velocity model via data processing and recognize synthetic seismic "marine" data wavefield propagation phenomena, such as velocities pull up under salt layers or velocities sagging, due to the presence of pore filling material (i.e., hydrocarbons). Although simple, we think that the results derived from the present model are valuable in terms of assessing general models (mainly velocity models) for such a kind of basins and also can be a starting point for future upgrades, enhancing the knowledge in processing and interpretation.

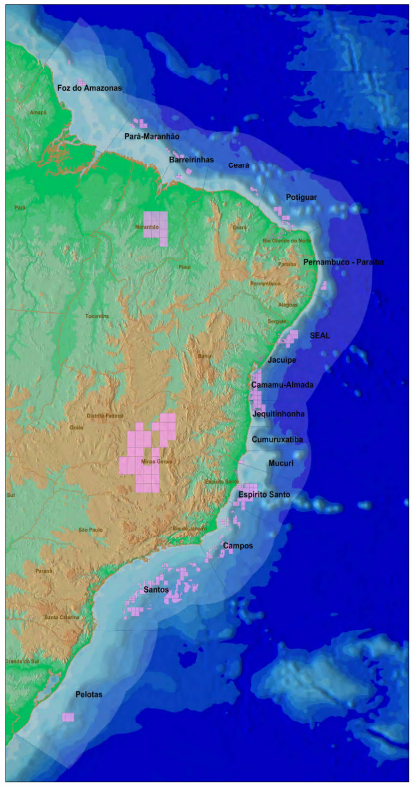

Figure 1—The Brazilian marginal basins.

The present presalt model continues to be updated, mainly to include the precise features of the carbonate rocks so far described in the sag/rift section. But the results we present here are representative enough to consider the main effects usually recognized in seismic marine data acquired over these basins.

Framework, stratigraphy and evolution of the Brazilian marginal basins (Ojeda, 1982)

According to Ojeda (1982), eight basic structural features are described in the Brazilian marginal basins, on the basis of faults and strata attitude. These features are synthetic untilted step-fault blocks, antithetic tilted step-

fault blocks, structural inversion axes, hinges with compensation grabens, homoclinal structures, growth faults with rollover structures, salt and shales diapirs, and structures related to igneous activities. Some of these features are characteristic along all Brazilian marginal basins, while others are described isolated or limited by some other feature. But all of them play an important role in the definition of prospective and nonprospective areas.

The synthetic untilted step-fault blocks are asymmetric features limited by normal faults, where the strata and the faults are both inclined basinward. The steep-dip downthrown blocks exhibits the distal sedimentary facies deeper than the proximal and synchronous ones. This structural-stratigraphic relationship developed concomitantly with the sedimentation related to descendant, vertical, differential movements that increase basinward. In some cases, there exists intermediate blocks that fell slower, forming intrabasinal horsts with thin sedimentary sections, sometimes partly truncated by erosion.

The antithetic tilted step-fault blocks are asymmetrical features, the strata of it inclined opposite to the depositional dip. The blocks are limited by antithetic faults, its planes dipping basinward. These structures developed concomitantly with the sedimentation. In the downthrown blocks, syntectonic conglomerates were deposited along the fault planes, the beds of it thinning towards the culmination of the tilted blocks.

The structural inversion axes are alignments that separate antithetic tilted and synthetic untilted step-fault blocks. It is believed to exist along the whole marginal Braziian basins, and it is most probably related to the definitive rupture of the Gondwana (Ojeda, 1982).

In the case of the hinges with compensation grabens, the dip of the strata is abruptly increased basinward, but it is not inverted in its original attitude. Generally, normal direct and antithetic faults develop adjacent or subparallel to the flexure line in areas of smooth dips. The asymmetric grabens are formed by accommodation of blocks to reestablish the regional tectonic stability, and it separates prospective ares from the shallow, nonprospective, areas.

Finally, the last of the diastrophic features to be commented are the homoclinal strtuctures. These represent a regional feature, widespread along the whole basins, and which overlain the taphrogenic structures and affect the post-Albian sediments. In the eastern coast it generally exhibits a smooth to steep dip. Overlying these features there exists continental and marine sediments, deposited as fan-delta, shelf and slope systems, prograding basinward.

Among the adiastrophic structural features, growth faults with associated rollovers are promising oil prospects. They are generally associated with the salt/shale mobilization, in which the rollover shows thinning of strata from the flank to the top of the structure, revealing sometimes synsedimentary growth of paleostructures. The growth structures constitute natural paths of migration of hydrocarbons, sometimes generated in evaporitic sequences or in pro-delta slope shales, and the hydrocarbons could end up trapped in younger structured reservoirs.

Salt and shale diapirs generally occur basinward as incipient pillows or well developed domes and walls. The pillows are overlain by quaquaversally arcuated strata and exhibit a concomitant sedimentation and structuralization, the strata of it thinning towards the apex of the structures. The deformed sediments are generally carbonates and deltaic deposits, which constitute excellent exploration targets for oil. The piercements of the domes are located along the outer trend of the basins, adjacent to rollovers and also to the pillows trend.

Finally there are magmatic and igneous structures. They are dome-like structures with quaquaversal to triversal closure, their nuclei formed by basaltic and andesitic dikes or sills.

Several authors (Milani et al, 1991) state that all these structures are distributed according to the location and their relationship with the evolution (i.e., the drifting) of the South American and African plates. They are distributed in subparallel and adjacent trends running from the border to the depocenter of the basins. The order is: border of the basins, hinges, synthetic untilted step-fault blocks, inversion axes and antithetic tilted step-fault blocks (Ojeda, 1982). The synthetic and antithetic step-fault blocks developed synchronously with the rift phase of the Gondwana continent (Early Cretaceous, running through the Neocomian, Barremian and possibly the Aptian). The structured strata are mostly clastic non-marine (fluvial, deltaic and lacustrine) with some local evaporites. The hinges are probably related to the drift of the continents during the Albian-Cenomanian. Here the main structured strata are composed of evaporites, marine clastics and carbonates. Finally the homoclinal structures, developed through the Early Cretaceous (Albian) to the Cenozoic, are overlain by marine sediments, deposited as fan-delta, platform and slope systems.

The tectonic-sedimentary evolution of the Brazilian marginal basins follows the sequence: crustal uplift (intumescence or pre-rift), rift phase (taphrogenic), transitional phase (evaporites) and drift phase.

The pre-rift phase (Late Jurassic to Early Cretaceous) includes local volcanic activity and a variable intensity along the what-would-be-called “margin”. In its peripheral basins (Ojeda, 1982), nonmarine fluvial-lacustrine sediments were deposited.

In the rift phase (Early Cretaceous to Late Cretaceous), intense tectonic activity formed asymmetric rift valleys and a central graben, with volcanic activity associated. The sedimentation here took place mainly in elongate lacustrine basins, with clastic, nonmarine, fluvial, deltaic and deep-water basinal deposits – the proximal and distal facies. Coarse to fine sandstones, silts and shales are the dominant lithologies, alongside with coarse conglomerates deposited along faults. Igneous activity occurred in this phase, affecting the Santos and Campos basins, as well as other basins.

The transitional phase includes the deposition of evaporites, some clastics and carbonates, under conditions of relative tectonic stability. This phase seems

to have occurred during the Aptian in two phases. In both phases there occurs the formation of a gulf, locally supplying marine waters to evaporitic basins located over the rift valleys. This phase of evaporite deposition is intermixed with the deposition of thick clastic fluvial-deltaic and lagoonal sediments. Later on, a regional marine transgression took place giving rise to an evaporitic cycle.

Finally, in the drift phase intense marine and nonmarine sedimentation occurred as a thick wedge of clastic-carbonate deposits (Ojeda, 1982).

Today, the most prominent and commercial production of hydrocarbons in the marginal basins is from fluvial-deltaic sandstones of the rift-valley lacustrine sequences, from fluvial fan-delta conglomeratic sequences underlying the evaporates, and calcarenites and turbidite sandstones of the marine sequence. The source rocks in the rift-valley lacustrine sequence are prodelta and basinal shales. Any hydrocarbons generated here probably migrated updip through faults, accumulating in shallow or adjacent structural traps associated with basinal horsts, or accumulated in local horsts in regional paleohighs and rollovers formed by growth faults.

In a general sense, the stratigraphic framework of the East margin basins thus is formed by four main sections: the basement; the pre-salt section (the rift and sag sections); the transitional section, where there exists a predominance of evaporites and carbonates; and the passive margin section, which includes the siliciclastic section. This nomenclature is to be followed in this paper.

In other regions such as in Santos basin, the layers of salt are very thick and completely seal the sediments underneath. In this case the most probable reservoirs, such as the ones in the Tupi area, are carbonate rocks (microbiolites).

Method

In order to represent (geophysically speaking) some of the tectonic-sedimentary features described in the last section, we have constructed a velocity model in depth. The geologic model we consider with its respective interval velocities is made of four sequences (**Figure 2**):

(I) the basement (6.5 Km/s);

(II) the presalt section (4.5 Km/s);

(III) the salt layer (5.5 Km/s);

(IV) the Tertiary-Upper Cretaceous section, with a constant velocity gradient v(z).

Above this stack of isotropic layers, there is a water layer (1.5 Km/s) with 2.0 Km of thickness. Totaling, disregarding the water layer, we have 6.0 Km of heterogeneous sediments in thickness. The basement is represented by a high in the form of a ramp, towards it a homogeneous presalt layer (presuming to contain altogether rift and sag strata) onlap onto. Right above this layer, we have placed a thick layer of salt (2.0 Km wide), with a horizontal bottom and the top displaying two isolated, asymmetric, domes, separating an isolated minibasin. Above the salt, the Tertiary-Upper Cretaceous section is believed to represent a thick and homogeneous siliciclastic section. Some unconformities present in the latter section is believed to be well represented by the $v(z)$ velocity profile.

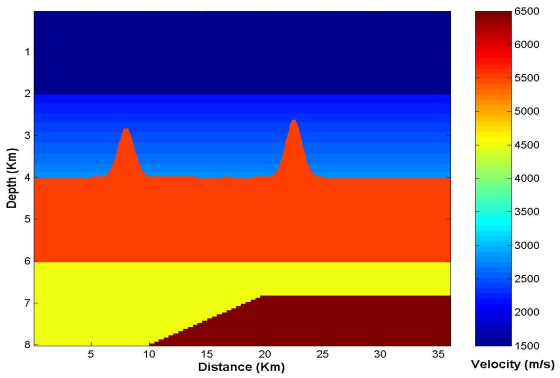

Figure 2 – Presalt depth velocity model.

The velocities in these layers were chosen so as to represent the impedance contrast commonly observed in marine seismic data. The water layer velocity is the most known and assessed value. In the Tertiary-Cretaceous section the most common velocity field is deph-dependent, i.e. $v(z)$, due to the predominant siliciclastic stack of sedimentary rocks. Here we considered as starting velocity v_0 the velocity at water bottom, with a constant gradient given by $\beta = 0.316\ s^{-1}$. Thus, right above the salt layer, the velocity value is 2.784 Km/s, at depth $z = 4.0$ Km.

The salt layer was chosen to be homogeneous with a constant velocity of 5.5 Km/s. This value is high enough to grant a large impedance contrast at the top and the bottom of the layer. That is why we have chosen as mean velocity for the sag and rift section the value 4.5 Km/s. One of the great challenges in seismic data processing for marine data is to image under salt layers or domes, due to the multipathing of seismic energy in these regions. In Brazil the salt is mostly autochthonous, giving rise to domes, pillows or (thick) sheets. In our model, we are most interested on the sheets of salt, and on its imaging effects right under a dome-like feature. In the latter, the most prominent feature is velocity “pull-up”. This feature in seismic data is responsible for the indetermination of the salt bottom, principally when dealing with time-migrated images.

Considering the chosen velocity model and its features described above, we have simulated a synthetic 2D seismic marine acquisition covering a region of 36 Km in space, with a total of 8 seconds of record. The geometry of geophones was end on, with a total spread of 0-25-8025 meters. Shots were located every 50 m, as well as the end on array had its geophones spaced every 25 m also. The first shot was acquired at position $x_S = 8.05$ Km, while the last shot was “fired” at position 36 Km, covering circa 27.95 Km.

We have chosen to acquire the simulated data using a common-offset approach, following the spread designed to the synthetic survey. In this case 85 common-offset

sections were “shot”. These sections represent a total as if 560 shots were fired with 340 active channels.

In a first hand, all interfaces are constructed using analytic function of the type $z = f(x)$, where z is the depth coordinate of the reflecting interface and x is its surface coordinate. Thus to represent the salt domes we have used inverted Gaussians. The basement high is partially constructed with constant function and a linear function, this latter with is specific gradient and intercept. The water bottom and the surface of the ocean are also linear functions.

For the synthetic modeling of the common-offset sections we have used the algorithm of Podvin and Lecomte (1991) to estimate traveltimes, which is based on the single solution of the eikonal equation (first arrivals only). The dynamic part of the wavefield (i.e., amplitudes) was obtained by the use of Kirchhoff modeling integral. Since the reflecting interfaces are determined by analytic functions, it is easy to implement a code that considers the interfaces as curves, i.e., functions of x (surface coordinates).

In the present example the density model was considered unity in the entire model. The V_P/V_S relation was set to 2, in principle, since we know that in a future update of the model this relation must be altered in order to consider other lithologies and bring its rock physics close to reality. We know that in dealing with carbonates, for example, the V_P/V_S ratio is nonlinear, and this ought to be taken in consideration.

As for the reflection coefficients, we have used the Aki and Richards (1980) isotropic equation for *PP* reflections:

$$R_{PP}(\theta) = A + B\,sin^2(\theta) + C\,sin^2(\theta)\,tan^2(\theta) \qquad (1)$$

in which the coefficients A, B and C each carry an specific contribution of V_P, V_S, density and Poisson impedance ratio that will not be shown here, only mentioned. These relations can be seen in several references (e.g., Aki and Richards, 1980; Shuey, 1985) and are well known. Since in a future update of this model the objective is to invert to AVO parameters, the choice of Eq. (1) will be of great value.

Examples

Figure 3 displays one common-offset section with $2h$ = 50 m. The main features observed are the good continuity of the flat and linear events, like the water line, the water bottom, parts of the bottom of the salt layer and the high of the basement and the ramp of the basement. On the top of the salt layer the well known diffractions on the flanks of the domes are representative. On the bottom of the salt layer, right under the salt domes, the most prominent features are the pull-ups caused by the great velocity impedance when the seismic wavefront passes through the salt and enters the underlying sediments, i.e., the presalt section. These pull-up events are also extensive to immediate underlying horizons, such as the top of the basement high. In all common-offset sections generated, this particular feature is always present, showing that the solution of the eikonal equation is effective in simulating this kind of features.

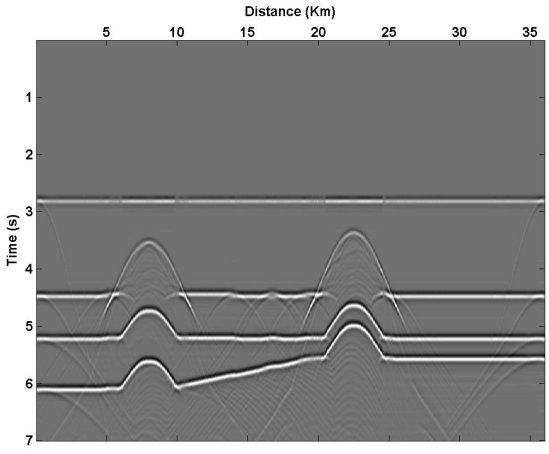

Figure 3 – Common-offset section (2h = 50 m) simulating a 2D seismic marine acquisition over the area of the velocity model in Figure 2.

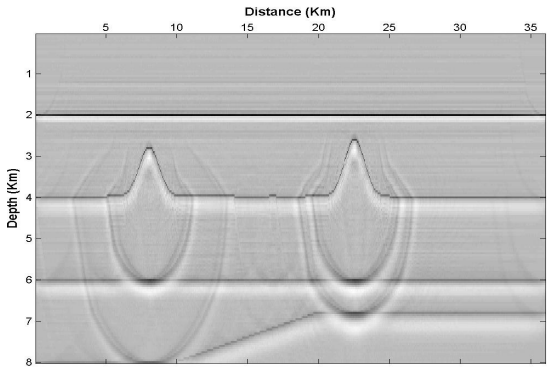

Figure 4 – Prestack depth migration of the $2h$ = 50 m common-offset section in Figure 3.

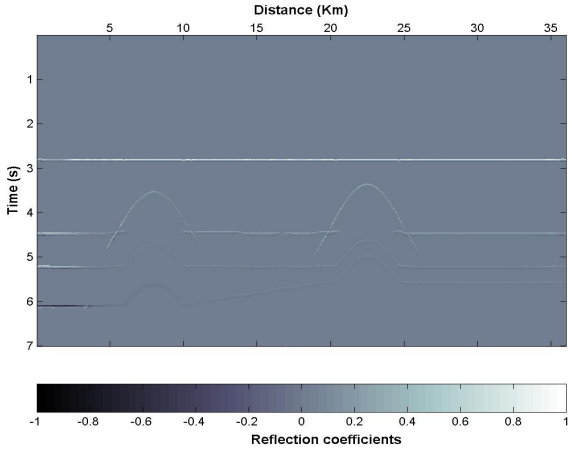

Figure 5 – Attribute section extracted from the common-offset section in Figure 3.

In **Figure 4** we show the result of the depth migration performed on the common-offset section of Figure 3. Since we have used the true velocity model, all events were correctly positioned in their true depth positions. This particular migration was performed using a Kirchhoff-like algorithm known as KGB-PSDM (Ferreira, 2006), where a Gaussian Beam operator (Červený, 2001) is used in the kernel of the main migration process. The algorithm was able to efficiently reconstruct the bottom of the salt layer, thus collapsing the pull-ups all along. The same occurred to the pull-ups observed on the top of the basement. The migration artifacts seen on the image are inherent to the process, and are completely eliminated in the stacking of all the common-offset migrated sections (not shown here).

In **Figure 5** we display the amplitudes along the reflectors estimated via a vector diffraction-stack technique (Hanitzsch, 1994), adapted for the modeling Kirchhoff integral used in this work.

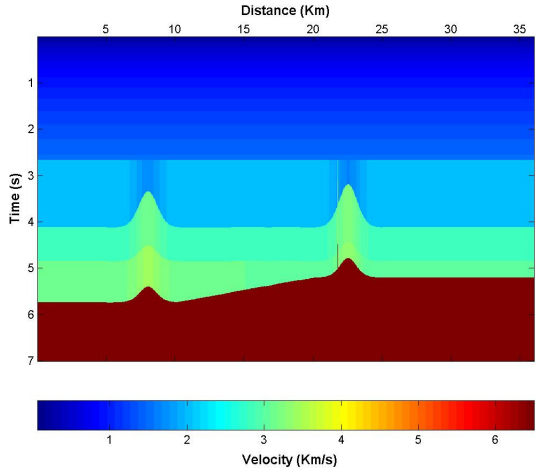

Figure 6 – Presalt time velocity model.

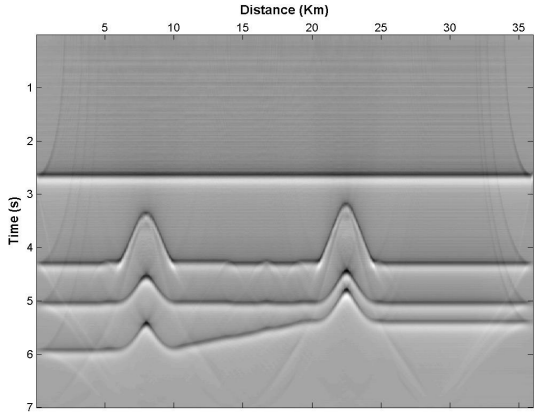

Figure 7 – Prestack time migrated section of the common-offset section in Figure 3.

Finally we have compared the result of the present depth migration process with a (Kirchhoff) prestack time migration. In order to do this, we had to estimate the velocity model in time using the Dix algorithm (Dix, 1955). **Figure 6** shows the velocity model obtained with this technique. After that, we have time migrated (Alkhalifah, 2006) the same data with this specific velocity model. The result is displayed in **Figure 7**. As expected, all the pull-ups were not collapsed, since time migration in general is not able to do it.

Like the depth migrated section (**Figure 4**), migration artifacts (smiles and border effects) are present all over the section. They are inherent to the migration process and are coherently removed by the stacking of all the common-offset sections.

Conclusions

We have modeled a synthetic 2D seismic marine acquisition over a hypothetical presalt prospect representative of subsurface profiles found in the Brazilian East margin basins. The starting model considered only four main sections, representing mega-sequences of strata: the basement, the presalt section (which includes two separates depositional sequences, the rift and sag sections), passing through one thick salt section and ending up with an Upper Cretaceous-Tertiary siliciclastic section right under the water bottom.

Over this geological model, we have established a depth velocity model that served as input for a synthetic 2D seismic common-offset acquisition that used the eikonal equation to estimate the traveltimes and the Kirchhoff modeling integral to calculate amplitudes. The reflection coefficients were determined using the Aki and Richards (1980) equation for *PP* waves. The seismic interfaces are represented by analytical functions of the surface positions, such that linear functions and Gaussian functions are used in order to represent planes and salt domes.

The synthetic seismic data obtained correctly predicted all propagation effects that are seen under salt, for example, with velocity pull-ups being located under the salt domes, exactly in the same manner as it happens in real seismic. These pull-ups are also extensive to all other features directly under the salt domes, such as parts of the basements. In this example, these pull-ups introduce challenging situations for data processing.

We have performed a Kirchhoff-like prestack depth migration using the KGB algorithm (Ferreira, 2006). This process correctly positioned all reflections in its true depth positions and collapsed all diffractions. The pull-ups were also completely collapsed, so that the bottom of the salt layer was correctly reconstructed, as well as all the others features affected by the impedance contrast. As a co-product, the amplitudes along the horizons of interest were effectively picked via a vector diffraction stack procedure during migration (Hanitzsch, 1994).

The occurrence of pull-ups was also investigated for the case of prestack time migrated. A time velocity model was obtained with the use of the recursive algorithm of Dix (1955) and a Kirchhoff prestack time migration was performed. As expected, time migration was not able to

position the pull-ups reflections in its true spatial positions in depth.

We conclude the present work with the news that the present model is being updated in order to include specific and more accurate characteristics of the geological profiles commonly found in the Brazilian East margin offshore basins. This present development of the geological model aims future studies of seismic inversion (acoustic and elastic), rock modeling, AVO/AVA analysis and anisotropic imaging. We are particularly interested in extend the present analysis to the study of carbonate reservoirs, in which recent discoveries were announced in the exploration block BM-S-11 (ANP nomenclature) in a prospect historically named Tupi.

Acknowledgments

The authors would like to thank Agência Nacional do Petróleo (ANP/Brazil) for the permission to publish this work and for making available the workstation environment at Exploration Superintendence (SEP) in its headquarter in Rio de Janeiro, where all the numerical results of this paper were developed. In particular, A. S. O would like to thank Ana Cláudia de Góes Lopes (ANP/SDT), for the valuable help with the GIS software.

References

Alkhalifah, T., 2006. Kirchhoff time migration for transversely isotropic media: An application to Trinidad data. Geophysics (**71**): S29-S35.

Aki, K.; Richards, P., 1980. Quantitative seismology – Theory and methods, vol. 1: W. H. Freeman and Co.

Červený, V., 2001. Seismic ray theory: Cambridge Univ. Press.

Dix, C. H., 1955. Seismic velocities from surface measurements. Geophysics (**20**): 68-86.

Ferreira, C. A. S., 2006. Migração Kirchhoff pré-empilhamento em profundidade modificada usando o operador de feixes gaussianos. Universidade Federal do Pará, Tese de Doutorado.

Hanitzsch, C., 1994. Vector diffraction stack migration: A fast technique for amplitude preserving Kirchhoff migration. SEG Expanded Abastracts **13**, 1183.

Milani, E. J.; Brandão, J. A. S. L.; Zalán, P. V.; Gamboa, L. A. P., 1991. Petróleo na margem continental brasileira: geologia, exploração, resultados e perspectivas. Brazilian Journal of Geophysics (**18**): 351-396.

Ojeda, H. A. O., 1982. Structural framework, stratigraphy and evolution of the Brazilian marginal basins. AAPG Bulletin (**66**): 732-749.

Podvin, P.; Lecomte, I., 1991. Finite-difference computation of traveltimes in very contrasted velocity models: a massively parallel approach and its associated tools. Geophys. J. Int. (**105**): 271-284.

Shuey, R. T., 1985. A simplification of the Zoeppritz equation. Geophysics (**50**): 609-614.